

# Electrochemical detection of Gonadotropin-releasing hormone agonists for uterine fibroids based on Poly(L-Serine)/Ag NPs/GO nanocomposite modified glassy carbon electrode

Cong Zhou<sup>1</sup>, Jing Liu<sup>1,\*</sup>, Weiwei Zhuo<sup>2,\*</sup>

<sup>1</sup> Department of Obstetrics and Gynecology, Xiantao First People's Hospital Affiliated to Yangtze University, Xiantao, 433000, China

<sup>2</sup> Department of Pharmacy, Jiangsu Vocational College of Medicine, Yancheng, 224005, China

\*E-mail: [weiweiz999@126.com](mailto:weiweiz999@126.com), [bobobushimao810922@163.com](mailto:bobobushimao810922@163.com)

Received: 15 November 2021 / Accepted: 20 December 2021 / Published: 5 January 2022

In this work, an electrochemical sensor of Gonadotropin-releasing hormone (GnRH) agonists was proposed by deposition of the conductive nanocomposite of Ag and graphene oxide on glassy carbon electrode (Ag-GO/GCE) and electropolymerization of poly(L-Serine) on nanocomposite (p-L-serine/Ag-GO/GCE). Because of excellent conductivity between Ag nanoparticles and graphene oxide nanosheets, and synergic catalytic effect of Ag-GO nanocomposite and the conducting polymer, the developed GnRH sensor provides a highly porous surface and a larger effective surface area, which facilitates electron transfer and promotes the electro-catalytic performance. p-L-serine/Ag-GO/GCE exhibited good electro-catalytic and selectivity with a sensitivity of  $0.74036 \mu\text{A}/\mu\text{gml}^{-1}$ , a linear range of 1 to  $15 \times 10^7 \mu\text{g/ml}$ , and a low detection limit of 20 pg/ml ( $S/N = 3$ ). Moreover, the p-L-serine/Ag-GO/GCE was successfully applied for the determination of GnRH in real blood serum of patients aged 40-50 years old who administrated GnRH for treatment of uterine fibroids and the obtained  $RSD \leq 4.20\%$  was demonstrated to good accuracy of p-L-serine/Ag-GO/GCE for the determination of GnRH in patient blood serum and in clinical applications.

**Keywords:** Electrochemical sensor; Uterine fibroids; Gonadotropin-releasing hormone agonists; silver nanoparticles; graphene oxide; Poly(L-Serine); Amperometry

## 1. INTRODUCTION

Fibroids, also known as leiomyoma or myoma in medical terms, are muscular tumors that form in the uterine wall. Fibroids are virtually typically noncancerous and benign [1, 2]. Fibroids can develop as a single tumor or as a cluster of tumors in the uterus. Women in their 40s and early 50s are the most likely to get fibroids [3, 4]. Fibroids do not affect all women in the same way. Fibroids are difficult to live with for women who have problems. Some women experience discomfort and

excessive menstrual bleeding [5]. Fibroids can also impose pressure on the bladder, which causes frequent urination, or the rectum, which causes rectal pressure. Fibroids can lead the abdomen to grow if they become particularly large [6, 7]. Medications that modulate hormone levels may be used to shrink uterine fibroids in the treatment of uterine fibroids. GnRH agonists are hypothalamic decapeptide amides (pGlu-His-Trp-Ser-Tyr-Gly-Leu-Arg-Pro-Gly-NH<sub>2</sub>) that stimulate the pituitary's release of luteinizing hormone (LH) and follicle-stimulating hormone (FSH) and, like leuprolide, progesterone levels and cause estrogen to plummet [8]. Menstruation will finally stop and fibroids will diminish as a result of this treatment. GnRH is just a tropic peptide hormone produced by GnRH neurons in the hypothalamus and released. The peptide is belonging to family of gonadotropin-releasing hormones. In the hypothalamic–pituitary–gonadal axis, it is the first stage [9].

Signs and symptoms of hypoestrogenism, such as hot flashes, migraines, and osteoporosis, are adverse effects of GnRH agonists. In individuals on long-term medication, sleeplessness, decreased libido, headaches, acne, mood swings, vaginal dryness, increased breast size, decreased breast size, muscle pains, depression, and dizziness are common side effects [10]. As a result, the method of administration, dosage, and duration of treatment are critical and are determined by the size and quantity of fibroids. As a result, determining hormones inside the human body is critical, and many investigations have been carried using liquid chromatography [11], mass spectrometry [12], radioimmunoassay [13], plasmon resonance immunoassay [14] and electrochemical techniques [15-17] to determine hormones in pharmaceutical and clinical samples. Electrochemical approaches with low-cost instruments have proved their superiority in terms of quick reaction, time savings, and ease of operation. Furthermore, the ease with which electrodes can be miniaturized utilizing nanomaterials and nanocomposites improves sensor sensitivity and stability [18-20]. However, few studies were conducted for the determination of hormone levels in clinical samples, and most of these studies were conducted using modified gold nanostructured electrodes, which are not economical [16, 17, 21-25]. In addition, these sensors do not present sufficient accuracy and selectivity and they need the more studies. Therefore, this study was focused on electrochemical detection of GnRH as a treatment for uterine fibroids based on p-L-serine/Ag-GO/GCE as an affordable, highly accurate, and high selectivity sensor.

## 2. EXPERIMENTAL SECTION

### 2.1 Preparation of the nanocomposite

For cleaning the GCE surface, it was polished with alumina powder (99%, Merckmillipore, Germany) and subsequently rinsed with DI water, and ultrasonically cleaned with a mixture of ethanol (99%, Shandong S-Sailing Chemical Co., Ltd., China) and DI water. The cleaned electrode was dried at room temperature. A homogeneous mixture of 0.5 mg/ml GO (99%, Globalchemical Factory Co., Ltd., China), 10 mM AgNO<sub>3</sub> (99.0%, Sigma-Aldrich), and ammonia (25 wt.%) was prepared under magnetic stirring in a volume ratio of 10:20:1 [26], and the mixture was ultrasonically shaken to obtain an Ag-GO nanocomposite in a yellowish brown color solution. The resulted dispersed nanocomposite

was centrifuged at 2000 rpm for 10 minutes, and the pellet was collected and washed with deionized water, and followed by redispersing in 1 mL deionized (DI) water. Next, 100  $\mu$ L of the Ag-GO nanocomposite suspension was applied to the modification of the clean GCE surface. After drying the modified electrode at room temperature, the p-L-serine was electropolymerized on Ag-GO/GCE using cyclic voltammetry (CV) in an electrochemical workstation (CHI 660E, CHI Instruments, Shanghai, China) with a three-electrode system, which contained an Ag/AgCl electrode, a Pt wire electrode and an Ag-GO/GCE, and these three kinds of electrodes were used as reference, auxiliary and working electrode, respectively [27]. The electropolymerization was conducted in a 0.1 M phosphate buffer solution (PBS) (pH 5.0) containing 20 mM L-serine (99.0%, Sigma-Aldrich) after 20 consecutive potential sweeps between -2.1 and +2.4 V. 0.1 M PBS was made by combining 31 mM  $\text{NaH}_2\text{PO}_4$  (99.0%, Sigma-Aldrich) solution with 68 mM  $\text{Na}_2\text{HPO}_4$  (99.0%, Sigma-Aldrich) solution and adding 15.4 mg/ml NaCl (99%, Merckmillipore, Germany) [28]. Afterward, the modified electrode p-L-serine/ Ag-GO/GCE was repeatedly washed with DI water to remove soluble impurities and any physically adsorbed species.

## 2.2 Analysis of real samples

The human serum was collected from four female patients aged 40-50 years old who were donors to GnRH (Knight Pharmaceutical Industry USA, LLC) for the treatment of uterine fibroids in Guangdong Women & Children's Hospital (Guangzhou, Guangdong Province, China). The blood serum samples were collected after two hours of GnRH administration, and centrifuged at 1000 rpm for 10 minutes. The resulted supernatants were used to prepare 0.1 M PBS (pH 7.4) which as prepared real samples, was used for the determination of the GnRH via amperometric analyses at -0.15 V. The GnRH ELISA Kits (CSB-E06880h/GNRH1, detection range: 2.5 pg/mL to 100 pg/mL, detection wavelength: 450 nm, CUSABIO, China) were also applied for the determination of the GnRH content in patients' blood serum samples.

## 2.3 Structural characterization and electrochemical detection procedure

Morphological studies of the modified electrodes were performed by field emission scanning electron microscopy (FESEM, S5200, Hitachi High-Technologies Canada, Inc., Ontario, Canada). An X-ray diffraction pattern recorded on an X-ray diffractometer (PW 1710, Philips, 40 kV, 20 mA, with Cu K radiation ( $\lambda = 1.5418$ )) was used to analyze the crystalline structure of prepared nanomaterials. The electrochemical workstation was used to perform CV and amperometry measurements in 0.1M PBS pH 7.4 and 3 mM of  $\text{K}_3[\text{Fe}(\text{CN})_6]$  (99.0%, Sigma-Aldrich) containing 0.1 M KCl (99.0%, Sigma-Aldrich).

## 3. RESULTS AND DISCUSSION

The X-ray diffraction patterns of powder GO and Ag-GO nanocomposite are shown in Figure 1. As seen, the X-ray diffraction pattern of GO exhibits a strong peak at  $2\theta = 9.82^\circ$ , corresponding to

(001) plane graphite oxide [29]. The Ag-rGO nanocomposite shows four sharp peaks at  $2\theta = 38.11^\circ$ ,  $44.50^\circ$ ,  $64.47^\circ$  and  $77.57^\circ$ , corresponding to the formation of (111), (200), (220), and (311) planes of fcc phase Ag (JCPDS card No. 00-04-0783). This confirms the successful syntheses of the Ag-rGO nanocomposite.

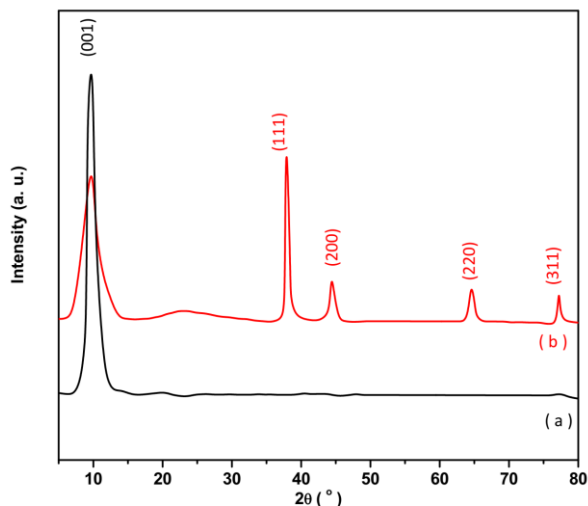


**Figure 1.** X-ray diffraction pattern of powders of (a) GO and (b) Ag-GO nanocomposite

In Figure 2, the FESEM images of modified electrodes were displayed. As is shown in Figure 2a, GO nanosheets drop on the GCE surface, indicating agglomerated blocks of folded and wrinkled sheets. In Figure 2b, the FESEM image of Ag-GO/GCE shows that the granular Ag nanoparticles cluster together and form spherical clusters, and the clusters are uniformly distributed on GO nanosheets on the GCE surface. Figure 2c also indicates the coverage of Ag-GO/GCE by p-L-serine because p-L-serine can be stabilized on the Ag-GO nanocomposite through interaction of its  $-NH$  groups with Ag nanoparticles and GO nanosheets [30, 31]. As a consequence, it changes the surface morphology of the modified electrode. As observed, both Ag-GO/GCE and p-L-serine/ Ag-GO/GCE show 3D porous networks.

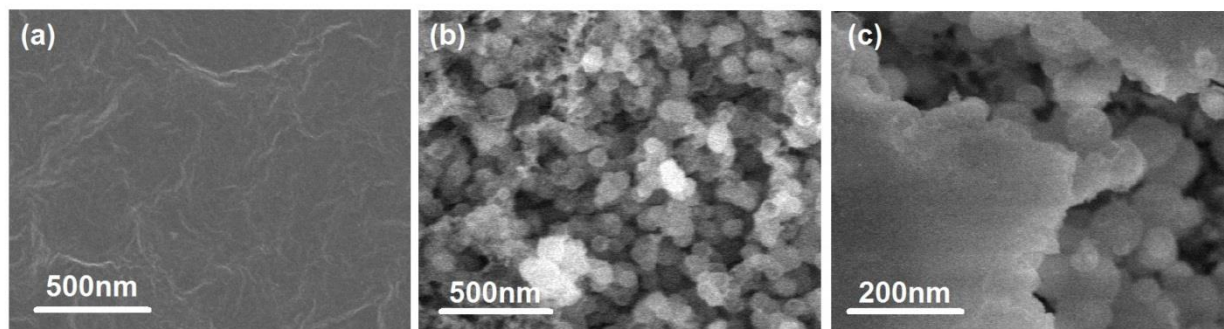


**Figure 2.** FESEM images of (a) GO/GCE, (b) Ag-GO/GCE, (c) p-L-serine/ Ag-GO/GCE.

Figure 3 depicts the CV responses of GCE, GO/GCE, Ag-GO/GCE and p-L-serine/Ag-GO/GCE in 3 mM of  $K_3[Fe(CN)_6]$  containing 0.1 M KCl as supporting electrolyte at scan rate of 20 mV/s. All electrodes exhibit a reversible redox reaction of  $[Fe(CN)_6]^{3-/4-}$  in solution, the separation between reduction and oxidation peaks is  $\sim 0.07V$  for GCE, and 0.06 V for GO/GCE, Ag-GO/GCE, p-L-serine/Ag-GO/GCE. The signal of CV responses of GCE is weak, while the current of electrochemical responses of p-L-serine/Ag-GO/GCE is about five-fold, three-fold and 1.5-fold higher than GCE, GO/GCE and Ag-GO/GCE, respectively. Thus, this observation illustrates the decrease in charge-transfer resistance and enhancement of the signal of electrochemical response with modification of the GCE surface, and the improvement of electrochemical current in p-L-serine/Ag-GO/GCE and Ag-GO/GCE is related to their 3D porous structures and enhancement of the electroactive surface area of electrodes [32, 33]. Furthermore, the excellent electrical conductivity of both Ag clusters and GO nanosheets promotes electrochemical response signaling [34, 35]. The good electrocatalytic activity of p-L-serine/Ag-GO/GCE demonstrates that it can be used for suitable electrocatalytic applications.

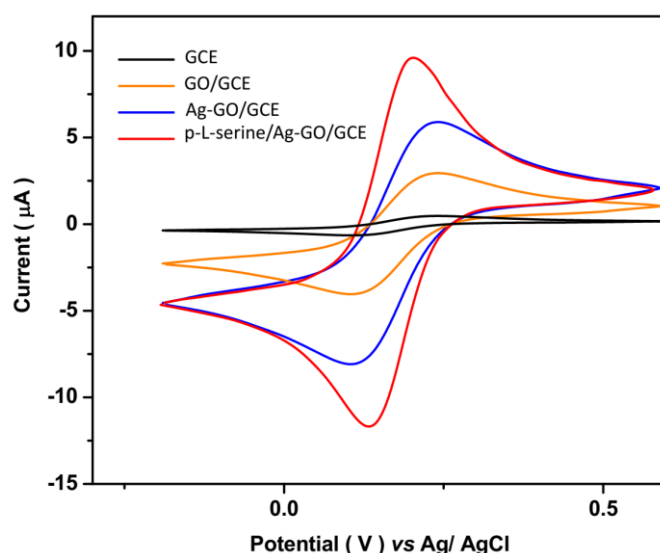


**Figure 3.** CV responses of GCE, GO/GCE, Ag-GO/GCE and p-L-serine/Ag-GO/GCE in 3 mM of  $K_3[Fe(CN)_6]$  containing 0.1 M KCl at scan rate of 20 mV/s.

Figure 4 shows the CV responses of all electrodes in 0.1 M PBS (pH 7.4) at a scan rate of 20 mV/s in the absence and presence of 1  $\mu\text{g/ml}$  GnRH. A comparison between the CV responses reveals that GCE and GO/GCE don't show any redox peak and only the background current is changed after the addition of 1  $\mu\text{g/ml}$  GnRH in solution. In the absence of GnRH, the CV curves of Ag-GO/GCE and p-L-serine/Ag-GO/GCE show the  $Ag^0/Ag^+$  redox peaks at 0.14 V and  $-0.19$  V for Ag-GO/GCE, and 0.14 V and  $-0.15$  V for p-L-serine/Ag-GO/GCE [36, 37]. After the addition of GnRH, the CV curves of Ag-GO/GCE and p-L-serine/Ag-GO/GCE show the increase in peak current at  $-0.19$  V and  $-0.15$  V, respectively, that is related to the reduction of GnRH. The lower peak potential and the higher

reduction peak current is occurred at p-L-serine/Ag-GO/GCE which can be related to interaction with functional groups on p-L-serine/Ag-GO/GCE with amino acids of GnRH [38, 39], as well as high porosity and great surface area, enhanced electron transfer kinetics and the presence of well-conductive Ag nanoparticles and GO nanosheets on the electrode surface [40, 41]. p-L-serine also causes some shifts in reduction potentials [42]. Therefore, further electrochemical studies were conducted on p-L-serine/Ag-GO/GCE.

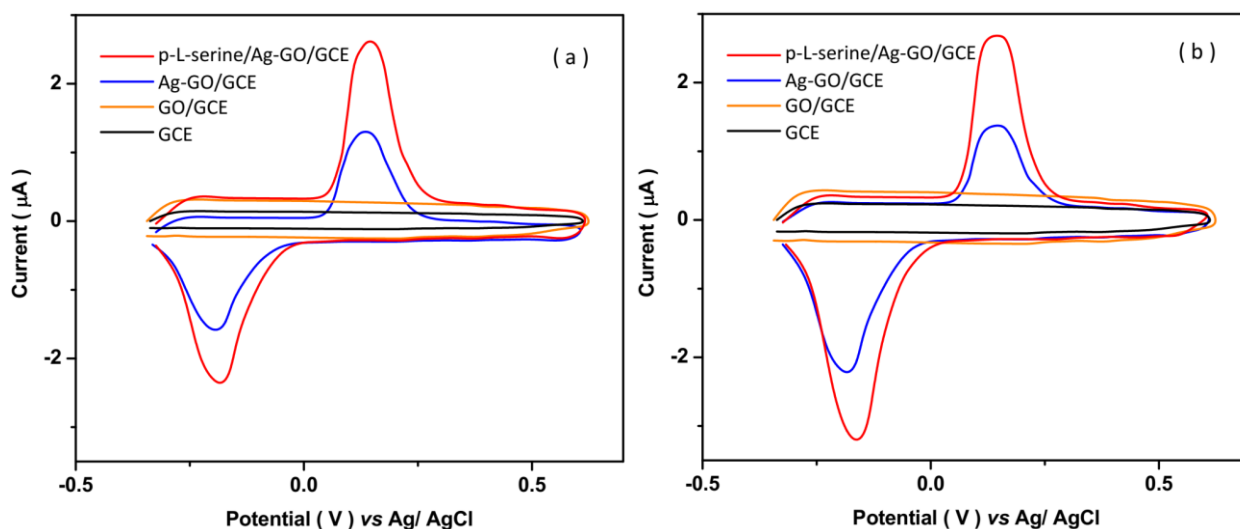


**Figure 4.** CVs responses of GCE, GO/GCE, Ag-GO/GCE, p-L-serine/Ag-GO/GCE in 0.1M PBS (pH 7.4) at scan rate of 20 mV/s in (a) absence and (b) presence of 1  $\mu\text{g/ml}$  GnRH.

An amperometry technique was utilized to determine GnRH at p-L-serine/Ag-GO modified GCE in 0.1M PBS (pH 7.4) at a potential of -0.15 V. It is shown in Figure 5a, that the electrocatalytic current of GnRH is linearly increased with increasing the concentration of GnRH in the range from 1 to  $15 \times 10^7$   $\mu\text{g/ml}$ . As seen from the calibration plots in Figure 5b, this linear relationship between the electrocatalytic current and the concentration of GnRH can be expressed with  $I(\mu\text{A}) = 0.74036 C_{\text{GnRH}} + 0.108783$  ( $R^2 = 0.99961$ ). Accordingly, the sensitivity is obtained at  $0.74036 \mu\text{A}/\mu\text{gml}^{-1}$  and the detection limit is 20  $\text{pg/ml}$  ( $S/N = 3$ ).

The interference, repeatability, and stability of p-L-serine/Ag-GO modified GCE were evaluated using an amperometry technique in 0.1M PBS (pH 7.4) at a potential of -0.15 V. Some salts, amino acids, and organic acids such as insulin, testosterone (TEST), lysozyme (LYZ), cortisol (CORT), ascorbic acid (ASA), estradiol (ESTR), immunoglobulin (IgG), ovalbumin (OVA), serum albumin (BSA),  $\text{Na}^+$ ,  $\text{K}^+$ ,  $\text{Cl}^-$ ,  $\text{PO}_4^{3-}$ , and  $\text{SO}_4^{2-}$  have been used as interfering substances to study their influence on the determination of GnRH.

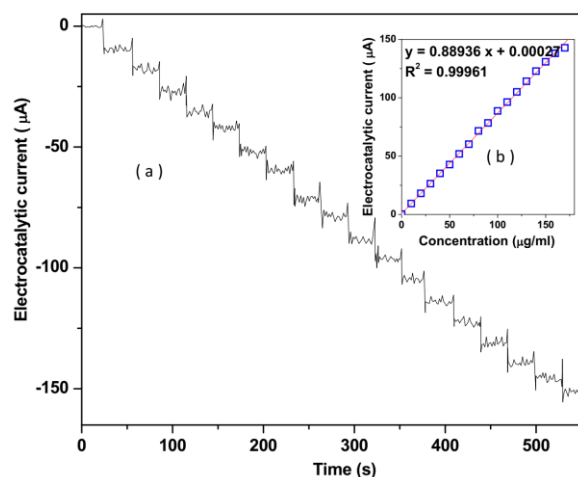


**Figure 5.** (a) Amperometry response of p-L-serine/Ag-GO modified GCE to addition of GnRH in 0.1M PBS (pH 7.4) at potential of  $-0.15$  V and (b) the related calibration plots.

As seen from Figure 6, the signal change for the addition of the 4-fold concentrations of interfering substances is much smaller than the created amperometric signals of additions of GnRH, indicating that these substances have no effect on GnRH detection. So, that is to say, the p-L-serine/Ag-GO/GCE shows high sensitivity and selectivity for the determination of GnRH. For the system electropolymerized with p-L-serin, the polymer molecules lying across the Ag nanoparticles and GO nanosheets and form a primary layer over the Ag-GO nanocomposite surface that selectively interacts with analyte molecules and thus shields them away from the nanocomposite surface and facilitates the stacking between analyte molecules [42, 43]. In addition, the value of the amperometric signals of the first addition of GnRH is very close to the value of the amperometric signals of the last addition of GnRH, which is demonstrated to have excellent repeatability and stability.

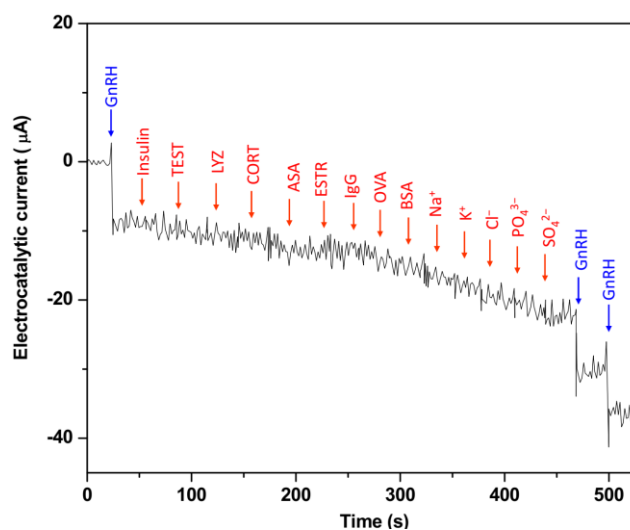


**Figure 6.** Amperometry response of p-L-serine/Ag-GO modified GCE to addition of 10 μg/ml GnRH and 40 μg/ml interfering substances in 0.1M PBS (pH 7.4) at potential of  $-0.15$  V.

Furthermore, the analytical performance of the proposed GnRH sensor is compared with the other reports on hormone detection from the literature, which are summarized in Table 1. These results implied that this developed GnRH sensor has a comparable and acceptable linear range and detection limit, which they attributed to the high conductivity of the p-L-serine/Ag-GO/GCE and the synergistic effect of Ag nanoparticles, GO nanosheets and the conducting polymer which facilitates electron transfer [9].

**Table 1.** Comparison between the analytical performances of the proposed GnRH sensor in this study with the other reports on hormone detection from the literature.

Electrode	Hormone	Method	Linear range (pg/ml)	Detection Limit (pg/ml)	Ref.
p-L-serine/Ag-GO/GCE	GnRH	Amperometry	$1-15 \times 10^7$	20	Present work
BSA/anti-hCG antibody/PANHS/SPCE	hGH	SWV	--	100	[15]
Chitosan/Au NPs/Graphene	hGH	EIS	100–2500	16	[16]
Anti-PTH/6-MHL/Au electrode	Parathyroid	EIS	0.1–0.6	0.001	[17]
Au-Pt hybrid disk electrode	Parathyroid	EIS	$1-10^5$	0.36	[21]
MoS <sub>2</sub> -Graphene/Au electrode	Parathyroid	CV	1–50	--	[22]
Au NPs/MWCNT/SPCE	Parathyroid	DPV	1–300	0.886	[23]
		SWV	1–300	0.65	
Poly(pyrrolepropionic acid)/MWCNTs	Prolactin	DPV	$10-10^7$	3	[44]
Poly(o-phenylenediamine)/Au NPs	Prolactin	DPV	0.05– $1.8 \times 10^5$	100	[45]
Au NPs/poly(ethylene-dioxythiophene)/CNTs/SPCE	Prolactin	DPV	$1-10^6$	0.22	[46]
	hGH	DPV	$50-10^6$	4.4	
mAbhHG antibody/tosyl-activated magnetic microparticles	hGH	SWV	$10-10^5$	5	[24]
Reversed-phase CN column	hGH	HPLC-HV	$5 \times 10^3-10^4$	2000	[47]
1,4-naphthoquinone/Ag/quinone	TSH	CV	$10^{-1}-10^5$	0.1	[48]
Antibody/Au NPs/ionic liquid/CPE	TSH	CV	$2 \times 10^3-9 \times 10^4$	100	[25]

BSA/anti-hCG/PANHS/SPCE: bovine serum albumin/antibody-human chorionic gonadotropin/1-pyrenebutyric acid-N-hydroxy-succinimide ester/screen printed carbon electrodes; hCG: human Chorionic Gonadotropin; Anti-PTH/6-MHL: Anti-parathyroid hormone/mercaptohexanol; hGH: human growth hormone; SWV: Square wave voltammetry; EIS: Electrochemical impedance spectroscopy; HPLC-HV: high-performance liquid chromatography with Hydrodynamic voltammetry; TSH: Thyroid stimulating hormone; CPE: Carbon paste electrode

The applicability and precision of p-L-serine/Ag-GO/GCE to the determination of GnRH were investigated in prepared samples of blood serum four patients aged 40-50 years old who were

administrated GnRH for the treatment of uterine fibroids. Figure 7 depicts the amperometry measurements and the resulting calibration plot of p-L-serine/Ag-GO/GCE to successive additions of GnRH solution in prepared 0.1 M PBS (pH 7.4) of blood serum at  $-0.15$  V. It illustrates that the GnRH concentration in the prepared sample of the first patient (S1) is 91.61  $\mu\text{g/ml}$ , which is very close to the obtained value by the GnRH ELISA kit (Table 2). These amperometry measurements were also performed for the other three samples and results of average of five ELISA assays and amperometry measurements for the determination of GnRH are displayed in Table 2. It can be found that there is good agreement between amperometry measurement and the corresponding ELISA assay. In addition, the obtained  $\text{RSD} \leq 4.20\%$  is demonstrated to have good accuracy of p-L-serine/Ag-GO/GCE for the determination of GnRH in blood serum of patients and for clinical applications.

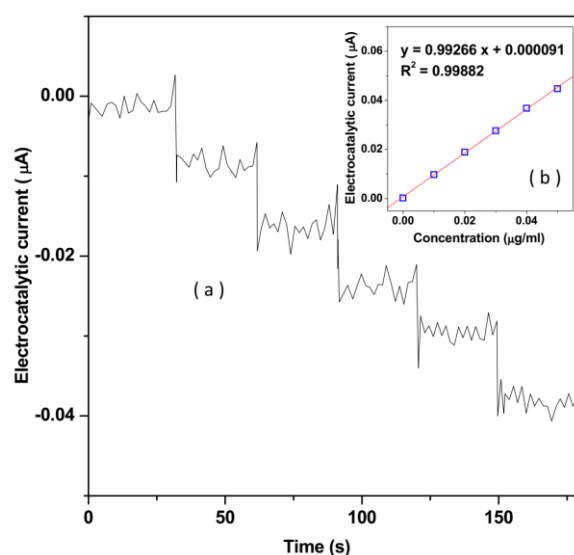


**Figure 7.** Amperometry measurements and resulted calibration plot of p-L-serine/Ag-GO/GCE to successive addition GnRH solution in prepared 0.1 M PBS (pH 7.4) of blood serum at  $-0.15$  V.

**Table 4.** The findings of determination of GnRH for prepared samples of blood serum 4 patients aged 40-50 years old using the ELISA kit and amperometry technique. The amperometry measurements conducted on p-L-serine/Ag-GO/GCE with successive addition GnRH in prepared 0.1 M PBS (pH 7.4) of blood serum at  $-0.15$  V.

Sample	Content of GnRH in prepared real serum sample ( $\mu\text{g/ml}$ )			
	Amperometry		GnRH ELISA kit	
	p-L-serine/Ag-GO/GCE	RSD (%)	ELISA	RSD (%)
S1	91.61	$\pm 3.58$	95.12	$\pm 3.15$
S2	88.22	$\pm 3.64$	86.69	$\pm 4.38$
S3	75.02	$\pm 4.20$	77.14	$\pm 4.05$
S4	80.72	$\pm 3.51$	81.879	$\pm 3.11$

#### 4. CONCOUSION

In summary, this work studied the performance of an electrochemical GnRH sensor based on p-L-serine/Ag-GO/GCE, which was fabricated by deposition of the conductive Ag-GO nanocomposite GCE and electropolymerization of p-L-serine on the nanocomposite. The successful synthesis of the Ag-rGO nanocomposite and the stabilization of p-L-serine on the nanocomposite surface were confirmed by structural and morphological studies. Electrochemical studies revealed good electrocatalytic performance and selectivity of p-L-serine/Ag-GO/GCE to determination of GnRH with a sensitivity of  $0.74036 \mu\text{A}/\mu\text{gml}^{-1}$ , a linear range of 1 to  $15 \times 10^7 \mu\text{g/ml}$ , and a low detection limit of 20 pg/ml ( $S/N = 3$ ). Furthermore, p-L-serine/Ag-GO/GCE was successfully applied for the determination of GnRH in real blood serum of patients aged 40–50 years old who were administered GnRH for the treatment of uterine fibroids, and the obtained  $RSD \leq 4.20\%$  was demonstrated to good accuracy by p-L-serine/Ag-GO/GCE for the determination of GnRH in patient blood serum and in clinical applications.

#### ACKNOWLEDGEMENT

The research was supported by the General Project of Natural Science Foundation of the Jiangsu Higher Education Institutions, Mechanism of  $\beta$ -catenin-mediated neuropeptide Y-induced cardiomyocyte injury (No. 20KJB310029).

#### References

1. Y. Orooji, B. Tanhaei, A. Ayati, S.H. Tabrizi, M. Alizadeh, F.F. Bamoharram, F. Karimi, S. Salmanpour, J. Rouhi and S. Afshar, *Chemosphere*, 281 (2021) 130795.
2. X. Tang, J. Wu, W. Wu, Z. Zhang, W. Zhang, Q. Zhang, W. Zhang, X. Chen and P. Li, *Analytical chemistry*, 92 (2020) 3563.
3. S. Okolo, *Best practice & research Clinical obstetrics & gynaecology*, 22 (2008) 571.
4. B. Zhao, X. Zhang, T. Yu, Y. Liu, X. Zhang, Y. Yao, X. Feng, H. Liu, D. Yu and L. Ma, *Acta Pharmaceutica Sinica B*, 11 (2021) 203.
5. X. Ji, C. Hou, Y. Gao, Y. Xue, Y. Yan and X. Guo, *Food & function*, 11 (2020) 163.
6. H. Maleh, M. Alizadeh, F. Karimi, M. Baghayeri, L. Fu, J. Rouhi, C. Karaman, O. Karaman and R. Boukherroub, *Chemosphere*, (2021) 132928.
7. A. Kvesić, D. Babić, D. Franjić, I. Marijanović, R. Babić and M. Martinac, *Psychiatria Danubina*, 32 (2020) 254.
8. R.E. Armer and K.H. Smelt, *Current medicinal chemistry*, 11 (2004) 3017.
9. W. Tang, S. Wan, Z. Yang, A.E. Teschendorff and Q. Zou, *Bioinformatics*, 34 (2018) 398.
10. M.A. Bedaiwy, C. Allaire and S. Alfaraj, *Fertility and sterility*, 107 (2017) 537.
11. M. Okano, M. Sato, A. Ikekita and S. Kageyama, *Rapid Communications in Mass Spectrometry*, 24 (2010) 2046.
12. J. Xu, L. Wu, W. Chen and A.C. Chang, *Journal of Chromatography A*, 1202 (2008) 189.
13. A.R. Midgley Jr and R.B. Jaffe, *The Journal of Clinical Endocrinology & Metabolism*, 26 (1966) 1375.
14. J. Treviño, A. Calle, J.M. Rodríguez-Frade, M. Mellado and L.M. Lechuga, *Talanta*, 78 (2009) 1011.

15. S. Damiati, C. Haslam, S. Sjøpstad, M. Peacock, T. Whitley, P. Davey and S.A. Awan, *IEEE Access*, 7 (2019) 94048.
16. S. Teixeira, N.S. Ferreira, R.S. Conlan, O. Guy and M.G.F. Sales, *Electroanalysis*, 26 (2014) 2591.
17. H.M. Özcan, K. Yildiz, C. Çakar, T. Aydin, E. Asav, A. Sağıroğlu and M.K. Sezgintürk, *Applied biochemistry and biotechnology*, 176 (2015) 1251.
18. Z. Savari, S. Soltanian, A. Noorbakhsh, A. Salimi, M. Najafi and P. Servati, *Sensors and Actuators B: Chemical*, 176 (2013) 335.
19. H. Savaloni, R. Savari and S. Abbasi, *Current Applied Physics*, 18 (2018) 869.
20. H. Savaloni, E. Khani, R. Savari, F. Chahshouri and F. Placido, *Applied Physics A*, 127 (2021) 1.
21. A.K. Yagati, A. Go, S.G. Chavan, C. Baek, M.-H. Lee and J. Min, *Bioelectrochemistry*, 128 (2019) 165.
22. H.-U. Kim, H.Y. Kim, A. Kulkarni, C. Ahn, Y. Jin, Y. Kim, K.-N. Lee, M.-H. Lee and T. Kim, *Scientific reports*, 6 (2016) 1.
23. G.-C. Chen, C.-H. Liu and W.-C. Wu, *Analytica Chimica Acta*, 1143 (2021) 84.
24. V. Serafín, N. Úbeda, L. Agüí, P. Yáñez-Sedeño and J.M. Pingarrón, *Analytical and Bioanalytical Chemistry*, 403 (2012) 939.
25. H. Beitollahi, S.G. Ivvari and M. Torkzadeh-Mahani, *Biosensors and Bioelectronics*, 110 (2018) 97.
26. A.a.M. Noor, M.M. Shahid, P. Rameshkumar and N.M. Huang, *Microchimica Acta*, 183 (2016) 911.
27. P. Naderi and F. Jalali, *Journal of The Electrochemical Society*, 167 (2020) 027524.
28. S. Kasemsumran, Y.-p. Du, K. Murayama, M. Huehne and Y. Ozaki, *Analyst*, 128 (2003) 1471.
29. M. Sharma, M. Patra and S. Jain, *Journal of Nanostructures*, 9 (2019) 547.
30. M. Li, F. Dang, Q.-L. Fu, D.-M. Zhou and B. Yin, *Environmental Science: Nano*, 5 (2018) 969.
31. C. Wang and Y. Jiang, *Journal of Physical Organic Chemistry*, 29 (2016) 69.
32. Y. Pan, K. Xu and C. Wu, *Nanotechnology Reviews*, 8 (2019) 299.
33. R. Savari, J. Rouhi, O. Fakhar, S. Kakooei, D. Pourzadeh, O. Jahanbakhsh and S. Shojaei, *Ceramics International*, 47 (2021) 31927.
34. R. Bhujel, S. Rai, K. Baruah, U. Deka, J. Biswas and B.P. Swain, *Scientific reports*, 9 (2019) 1.
35. F. Chahshouri, H. Savaloni, E. Khani and R. Savari, *Journal of Micromechanics and Microengineering*, 30 (2020) 075001.
36. L. Zhou, *International Journal of Electrochemical Science*, 16 (2021) 211043.
37. M. Vázquez, J. López, D. Medina-Rodelo, M. Jiménez-Edeza, G. Castañeda-Ruelas, A. López, J. Herrera-Ramírez and P. Méndez, *International journal of electrochemical science*, 14 (2019) 6366.
38. H. Shibaoka and K.V. Thimann, *Plant physiology*, 46 (1970) 212.
39. N. Magon, *Indian journal of endocrinology and metabolism*, 15 (2011) 261.
40. S.M. Naghib, E. Parnian, H. Keshvari, E. Omidinia and M. Eshghan-Malek, *International journal of electrochemical science*, 13 (2018) 1013.
41. R. Savari, H. Savaloni, S. Abbasi and F. Placido, *Sensors and Actuators B: Chemical*, 266 (2018) 620.
42. T. Sanglaow, P. Oungkanitanon, P. Asanithi and T. Sutthibutpong, *Molecules*, 26 (2021) 2876.
43. H. Savaloni and R. Savari, *Materials Chemistry and Physics*, 214 (2018) 402.
44. V. Serafín, L. Agüí, P. Yáñez-Sedeño and J. Pingarrón, *Sensors and Actuators B: Chemical*, 195 (2014) 494.
45. H. Chen, Y. Cui, B. Zhang, B. Liu, G. Chen and D. Tang, *Analytica Chimica Acta*, 728 (2012) 18.

46. V. Serafín, G. Martínez-García, L. Agüí, P. Yáñez-Sedeño and J. Pingarrón, *Analyst*, 139 (2014) 4556.
47. S.J. Choi, H.-Y. Lee, S.B. Kim, J.-H. Kim, S.S. Lee, S.D. Yoo, K.C. Lee and H.S. Lee, *Journal of Chromatography B: Biomedical Sciences and Applications*, 754 (2001) 461.
48. A. Bhatia, P. Nandhakumar, G. Kim, N.-S. Lee, Y.H. Yoon and H. Yang, *Biosensors and Bioelectronics*, 197 (2022)

© 2022 The Authors. Published by ESG ([www.electrochemsci.org](http://www.electrochemsci.org)). This article is an open access article distributed under the terms and conditions of the Creative Commons Attribution license (<http://creativecommons.org/licenses/by/4.0/>).